

CANCER

Functional Network Pipeline Reveals Genetic Determinants Associated with in Situ Lymphocyte Proliferation and Survival of Cancer Patients

Bernhard Mlecnik,^{1,2,3*} Gabriela Bindea,^{1,2,3*} Helen K. Angell,^{1,2,3} Maria Stella Sasso,^{1,2,3} Anna C. Obenauf,⁴ Tessa Fredriksen,^{1,2,3} Lucie Lafontaine,^{1,2,3} Amelie M. Bilocq,^{1,2,3} Amos Kirilovsky,^{1,2,3} Marie Tosolini,^{1,2,3} Maximilian Waldner,^{1,2,3,5} Anne Berger,⁶ Wolf Herman Fridman,^{2,3,7} Arash Raffii,⁸ Viia Valge-Archer,⁹ Franck Pagès,^{1,2,3,10} Michael R. Speicher,⁴ Jérôme Galon^{1,2,3†}

The tumor microenvironment is host to a complex network of cytokines that contribute to shaping the intratumoral immune reaction. Chromosomal gains and losses, coupled with expression analysis, of 59 cytokines and receptors and their functional networks were investigated in colorectal cancers. Changes in local expression for 13 cytokines were shown. Metastatic patients exhibited an increased frequency of deletions of cytokines from chromosome 4. Interleukin 15 (*IL15*) deletion corresponded with decreased *IL15* expression, a higher risk of tumor recurrence, and reduced patient survival. Decreased *IL15* expression affected the local proliferation of B and T lymphocytes. Patients with proliferating B and T cells at the invasive margin and within the tumor center had significantly prolonged disease-free survival. These results delineate chromosomal instability as a mechanism of modulating local cytokine expression in human tumors and underline the major role of *IL15*. Our data provide further mechanisms resulting in changes of specific immune cell densities within the tumor, and the importance of local active lymphocyte proliferation for patient survival.

INTRODUCTION

Global analysis of colorectal cancers (CRCs) has revealed the importance of adaptive immune cells for cancer patient survival. In particular, the nature, functional orientation, density, and location of immune cells within the tumor microenvironment were essential parameters, with a prognostic value superior to the tumor-node-metastasis (TNM) classification (1–3). Within the tumor microenvironment, the complex crosstalk between the tumor cells and the immune infiltrates involves cytokines (4), which are secreted or membrane-bound proteins involved in the recruitment of leukocytes from circulation to local inflammatory sites (5), and regulation of growth, differentiation, and activation of immune cells (6). They allow the maintenance of a stable equilibrium in the mature hematopoietic compartment (7), facilitate the recognition of tumor cells by the immune system (8), and inhibit tumor development and progression. Within tumor masses, T cell activation and differentiation were recently demonstrated (9). The mixture of cytokines produced in the tumor microenvironment may influence the immune infiltrates and thus contribute to sculpting the immune reaction of the host (10). On the other hand, host-derived cytokines could promote growth, attenuate apoptosis, and facilitate invasion and metastasis of tumor cells (6, 11). Through their cytokine production, tumors could manipulate the local microenvironment to escape immune surveillance (12).

¹INSERM UMRS1138, Laboratory of Integrative Cancer Immunology, Paris F-75006, France. ²Université Paris Descartes, Paris F-75006, France. ³Cordeliers Research Centre, Université Pierre et Marie Curie Paris 6, Paris F-75006, France. ⁴Institute of Human Genetics, Medical University of Graz, Graz A-8036, Austria. ⁵University of Erlangen-Nuremberg, Erlangen G-91054, Germany. ⁶Assistance Publique-Hopitaux de Paris, Department of General and Digestive Surgery, Paris F-75015, France. ⁷INSERM UMRS1138, Team 13, Paris F-75006, France. ⁸Stem Cell and Microenvironment Laboratory, Weill Cornell Medical College in Qatar, Education City, Qatar Foundation, Doha Q-10065, Qatar. ⁹MedImmune, Cambridge CG21 6GH, UK. ¹⁰Department of Immunology, Georges Pompidou European Hospital, Paris F-75015, France.

*These authors contributed equally to this work.

†Corresponding author. E-mail: jerome.galon@crc.jussieu.fr

An immunoscore, based on the enumeration of cytotoxic and memory T cells, both in the center and in the invasive margin of tumors, was previously described (13–15) and was shown to be a very powerful marker to predict patient outcome at all cancer stages (1–3). For instance, CRC patients with a strong immune reaction (I4) have a mean survival of more than 15 years, those with an intermediate immune reaction (I2) have a mean survival of about 5 years, and patients with a low immune reaction (I0) will survive less than 2 years (2). Given these major differences, it is essential to understand the mechanisms associated with high or low densities of intratumor adaptive immune cells.

We previously showed a strong correlation between interferon- γ (*IFNG*), a cytokine critical for tumor control, and T helper 1 (T_H1)-associated genes, with beneficial effect on the outcome of CRC patients (1, 16). In contrast, interleukin 8 (*IL8*), *IL10*, *TGFB1*, and other inflammatory and immunosuppressive genes showed no correlation with tumor recurrence. During the development and progression of cancer, genomic alterations (copy number variation) occur, which are likely to include genes favoring neoplastic progression (17). In particular, these alterations could affect cytokine family genes and subsequently modulate the local global cytokine expression.

Here, we studied cytokine and cytokine receptor copy number variations in a large cohort of CRCs to delineate mechanisms associated with cytokine expression. Our comprehensive analysis determined whether alterations of cytokine function contribute to tumor progression and how cytokines are shaping the intratumoral immune reaction.

RESULTS

Genomic alterations of the cytokines in CRCs

We investigated 59 soluble and membrane-bound proteins from the following cytokine families: IFN, IFN receptor (IFNR), IL, IL receptor

(ILR), transforming growth factor (TGF) superfamily, and tumor necrosis factor (TNF) superfamily (table S1). Many cytokine genes are placed in chromosomes 1, 5, and 9, and none is located in chromosomes 13, 14, 15, 17, 18, and 20. The genomic organization of cytokines revealed clusters of genes belonging to the same family, as previously described (18–21). Aberrations affecting an extended genomic region could therefore affect the entire cytokine clusters. The genomic profile of 109 CRC tumors (cohort 1) was investigated by array comparative genomic hybridization (aCGH). The frequency and the amplitude in the cohort of the genomic alterations were used to calculate the amplification and deletion scores. Gains on chromosomes 7, 8q, 13q, and 20 and losses on chromosomes 4, 8p, 14q, 15q, 17p, 18, 20p, and 22q, previously known to be associated with CRC, were identified (Fig. 1A) (22–24).

Each cytokine presented both losses and gains in different patients, but the frequency of those alterations within the cohort was low. Most patients did not have alterations of cytokine genes. The aberration profile was similar in different cytokine families (Fig. 1B and table S2). Patients without genomic alterations represented more than 75% of the cohort for each cytokine family. More than 10% of the patients presented a gain in TNF, IFN, IL, and TGF families. In contrast, TNF was the only family deleted in more than 10% of the cohort. The aberration profiles also reflected the chromosomal localization of cytokines. For example, members of the IL family were located on multiple chromosomes, and the frequency of their aberrations differed. ILs placed in chromosomes 1, 2, 5, 6, 7, 8, 11, 12, 16, and 19 had a higher frequency of gain than of loss. In contrast, ILs located on chromosomes 4 were mostly deleted. The amplitude of the cytokine aberrations varied in the cohort. The highest level of gain and loss (log ratio >0.5) was found for *IL29* and *IL15*, respectively. The highest frequency of gain and loss, respectively, was shown by *IL6* and *IL28RA* (Fig. 1B). These cytokines were located at 7p21 and 1p36.11, regions known to harbor aberrations in many cancer types (22, 25). Besides chromosome 7, the most frequent (>15% of the cohort) locations of amplified cytokines were in chromosomes 12, 16, and 19. Frequently deleted cytokines were located in chromosomes 1, 4, and 22. The magnitude of the cytokine aberrations also varied in the cohort. The highest level of gain and loss (log ratio >0.5) was found for *IL29* and *IL15*, respectively. An overview of the chromosomal location of the cytokines and their corresponding frequencies of gain/loss is illustrated in Fig. 1C.

Genomic alterations of cytokines and tumor progression

To facilitate exploratory analyses of large-scale data, we developed CluePedia (26), a ClueGO/Cytoscape plug-in (27–33). CluePedia integrates experimental and in silico data and was used to summarize the biological role of cytokine genes, as revealed by Gene Ontology (GO), KEGG, and Reactome. Figure 1D shows GO terms and pathways functionally grouped and their associated cytokine genes. The 59 cytokines and cytokine receptors investigated were involved in cytokine-cytokine receptor interactions, the JAK-STAT signaling pathway, hemopoietic or lymphoid organ development, cellular response to cytokine stimulus, regulation of response to stress, and regulation of cell proliferation.

At the tumor site, in addition to their role as chemoattractant, inhibitor, or activator of leukocytes, cytokines can also act as potential regulators of cancer cell transformation, growth, angiogenesis, and metastasis. We therefore investigated the relationship between cytokine gene copy number variation and the pathological progression or clinical stage of

CRC. We found a similar profile of genomic aberrations in tumor stages T1, T2, T3, and T4 (Fig. 1E). Patients without lymph node metastasis (N0) had significantly more amplification of *IL29*, *IL12RB1*, *TGFB1*, *TNFRSF1B*, *IFNAR1*, *IFNAR2*, and *IL10RB* than those with lymph node invasion (N1). Patients without distant metastases (M0) had significantly more *IL23A* amplifications compared with metastatic patients (M1). T and M stages were not significantly associated with an overrepresentational gain of any cytokine gene. In contrast, M1 patients displayed significantly more deletion of ILs: *IL2*, *IL8*, *IL15*, and *IL21* (Fig. 1F and table S3). Cytokines with an overrepresentation of gains and losses in N and M stages are marked on the network (Fig. 1D). Thus, no differences in genomic alterations of cytokines were associated with T stage, whereas patients with distant metastases had higher frequency of cytokine deletions.

Genomic alterations, cytokine expression, and clinical implications

The expression pattern of cytokines within CRCs was investigated using quantitative real-time polymerase chain reaction (PCR) (qPCR) in the 109 CRC tumors (Fig. 2). The genomic alterations occurring in tumor cells could provoke changes in local cytokine expression. To evaluate this hypothesis, we compared the expression of cytokines between patients harboring gain or loss and patients without copy number variations. We found 13 cytokines and receptors with significantly different expression in patients with aberrations (Fig. 2, A and B, and table S4). Nine cytokines and receptors, including members of the IFN family (*IFNA1*, *IFNA2*, *IFNA6*, *IFNAR1*, *IFNAR2*, and *IFNGR2*) as well as *IL2*, *IL21*, and *TGFB1*, showed significantly higher expression in patients having gain. Genomic deletions were associated with significantly lower expression of *IFNAR1*, *IL10RB*, *IL9*, and *IL15*. Examples of cytokine expression level in patients with gain and loss compared to those without aberrations are shown in Fig. 2C.

Next, we examined the relationship between cytokine genomic aberration and risk to relapse as a clinical outcome. We stratified patients into groups on the basis of their genomic profile (gain, loss, or no aberration). Log-rank analysis, comparing patients with and without genomic alterations, revealed four cytokines conferring a significantly different risk to relapse when deleted (Fig. 2B and table S4). None of the cytokine gains had an impact on relapse risk. However, patients with deletion of *IL15*, *IL2*, and *IL21* showed a higher risk to relapse compared to those without deletion. In contrast, patients with *IL12RB1* deletion had a lower risk to relapse. Among these four cytokines, only *IL15* showed a concordant significantly lower expression in the deleted group. Figure 2A shows the *t* test and log-rank significant cytokines and their functions: the regulation of metabolic process, of the response to stimulus, of the multicellular organismal process, and of the response to other organism, signal transduction, and leukocyte activation. The network was enriched with the chromosomal location and genomic alteration data.

IL15 at the tumor microenvironment: Interactions and in situ impact on immune cell proliferation

Within the tumor microenvironment, both infiltrating immune cells and tumor cells could be involved in cytokine production. Using publicly available data from the immunome compendium (34), we investigated which immune subpopulations are producing *IL15* (fig. S1). Activated dendritic cells and macrophages as well as B cells produced high levels of *IL15*. One of the *IL15* receptors, *IL15RA*, was expressed on the same cells as *IL15*. The other receptor, *IL2RB*, was expressed on cells with cytotoxic properties

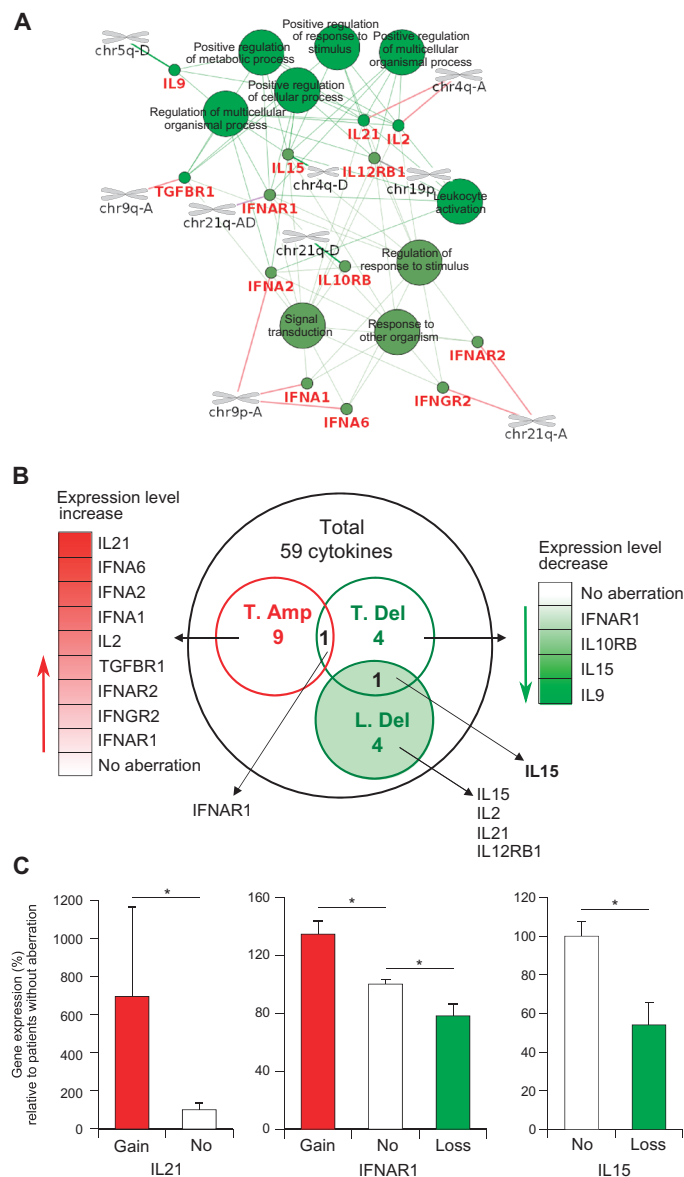


Fig. 2. Genomic alterations and the cytokine expression. The cytokine expression and the disease-free survival (DFS) were compared in groups of patients with gain or loss versus patients without aberrations. $P < 0.05$ was considered significant. **(A)** Thirteen *t*-test and/or log-rank test significant cytokines were analyzed using CluePedia. Pathways and functions of cytokines grouped on the basis of shared genes are shown as circular nodes. The links between the nodes are based on κ score. Cytokines associated to each function are shown. The chromosomal location and the aberration (A, amplification; D, deletion) are shown for each cytokine. **(B)** Venn diagram showing the number of *t*-test and log-rank test significant genes among the 57 cytokines. Thirteen *t*-test significant cytokines with gain (red) and/or loss (green) and their expression level increase/decrease compared to patients without aberrations are shown on the left and right, respectively. *IFNAR1* is *t*-test significant amplified and deleted. *IL15* deletion is log-rank and *t*-test significant. **(C)** Histograms representing the mean gene expression for *IL21*, *IFNAR1*, and *IL15* (relative to patients without aberrations) ± SEM. Gain, loss, and no aberration patient groups are shown in red, green, and white, respectively. Significantly different expression is marked by "*."

[CD8 T cells, T follicular helper cells, $\gamma\delta$ T cells, and natural killer (NK) cells] and on T central and effector memory cells and T_H1 and T_H2 subsets. Analysis of 176 cell lines (35, 36) showed that *IL15* is expressed by tumors from all the nine cancer types investigated.

IL15 production within the tumor microenvironment was analyzed immunohistochemically in patients with or without *IL15* deletion (Fig. 3A). The intensity of *IL15* was significantly lower in patients with *IL15* deletion (Fig. 3B). Patients with *IL15* deletion had a significantly higher risk to relapse compared to those without aberrations (Fig. 3C). We further demonstrated that *IL15* is produced by tumor cells, as illustrated by in situ hybridization (Fig. 3D), *IL15*, AE1AE3, and CD3 enzymatic double-stain combinations (Fig. 3E), and immunofluorescence triple staining (Fig. 3F).

The role of *IL15* was investigated using CluePedia. Functional terms were integrated into a network with in silico information and expression data from 105 CRC tumors (cohort 2) (Fig. 3G). The top 10 genes known to interact with *IL15* are cytokines and cytokine receptors: *IL2*, *IL4*, *IL7*, *IL21*, *IL2RA*, *IL2RB*, *IL2RG*, *IL15RA*, *IFNG*, and *TNF*. In contrast, CluePedia revealed that within the tumor microenvironment, *IL15* expression correlates mostly with *GZMA*, *HLA-E*, *GBP2*, *GBP4*, *KIAA0907*, *RAB8B*, *SAMD19*, *SP100*, *SNX10*, and *TNFSF13B*. Furthermore, as revealed by the network, *IL15* expression could be modulated by 3' untranslated region (UTR)-binding microRNAs (miRNAs): miR-130, miR-130b, miR-140-5p, miR-144, miR-148a, miR-148b, miR-152, miR-450b-5p, miR-891b, and miR-922. Finally, functional analysis showed that *IL15* is involved in extrathymic T cell selection, *IL17* production, positive regulation of proliferation and differentiation of NK cells, as well as proliferation of NK and T cells. The hypothesis that *IL15* is involved in the T cell proliferation was further experimentally validated by quantifying the proliferating T ($CD3^+Ki67^+$) cells in CRC tumors (Fig. 3H). Patients with deletion of *IL15* had a significantly lower density of proliferating T cells in the invasive margin compared to those without *IL15* deletion. A similar trend was observed in the tumor center. There was no difference in the T cell proliferation measured in the lymphoid islets in tumors with or without *IL15* deletion. The densities of tumor-infiltrating immune cells vary considerably from patient to patient, as illustrated for $CD3^+$ cells in Fig. 4 (A and B). Increased densities of T cells could be a reflection of an increased capacity of these cells to proliferate, potentially influenced by local cytokine production. We investigated this hypothesis by analyzing the density of adaptive and innate immune cell markers in groups of patients with different levels of *IL15* expression. Patients with high *IL15* expression had a significant increased density of T, cytotoxic T, activated T/NK, T_H1 , and memory T cells compared to those with low *IL15* expression (Fig. 4C). In contrast, no difference was observed in the neutrophil, mast cell, T_H17 , and NKp46 infiltrates. Additionally, patients with high *IL15* expression showed a significant increased expression of effector T cell markers (*GZMA*, *GZMH*, and *GZMK*), cytotoxic molecules (*PRF1* and *GNLY*), and T_H1 genes (*IFNG*) (Fig. 4D). Concordantly, high level of *IL15* expression was associated with a significantly lower risk to relapse compared to patients with low *IL15* (Fig. 4E). To demonstrate the importance of *IL15* expression in the general population of CRC patients, we excluded patients with *IL15* deletion. Similar results were obtained (Fig. 4F).

FACS analysis of the proliferation status of $CD3^+$ cells, isolated from fresh CRC tumor tissue, was performed under different conditions and illustrated as the number of proliferation cycles or the percentage of T cell proliferation (Fig. 3G). The number of proliferating T cells ($CFSE^+CD3^+$) significantly increased after $CD3/CD28$ stimulation for 5 days, indicating

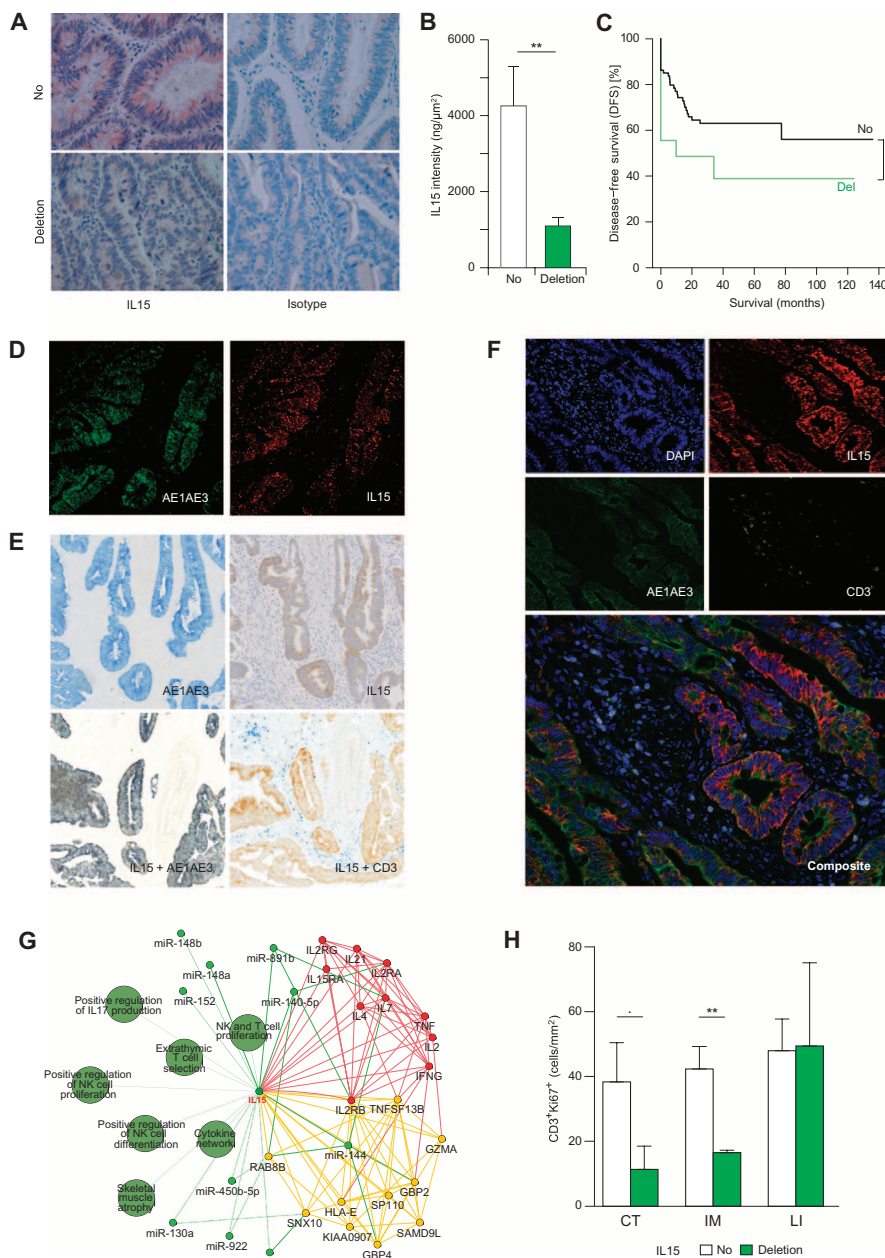
that intratumor T cells can be activated through T cell receptor stimulation. Five-day incubation with IL15 alone also induced the proliferation of intratumor T cells *ex vivo*. An augmented effect on the number of cycles of T cell proliferation, and thus the T cell proliferation percentage, was observed when IL15 was combined with CD3/CD28 stimulation.

IL15 expression level and immune cell proliferation in CRCs

We further investigated the impact of *IL15* on immune infiltrates from CRC tumors in situ (cohort 3). *IL15* has demonstrated chemotactic activity toward CD4 and CD8 T cells (37) and has been shown to induce T and B cell proliferation (38). We hypothesized that *IL15* expression level within CRC tumors could influence the proliferation of locally infiltrat-

ing immune cells. Using four-color fluorescence immunohistochemistry, we investigated and quantified the density (cells/mm²) of the in situ proliferation of T and B cells within different tumor regions (lymphoid islets, invasive margin, and center of the tumor) (Fig. 5). Triple staining allowed the quantification of proliferating B (CD20⁺Ki67⁺) and T (CD3⁺Ki67⁺) cells (Fig. 5A). Patients with high levels of *IL15* in lymphoid islets (Fig. 5B) and in the invasive margin (Fig. 5C) showed a significantly higher density of proliferating T cells compared to those with low levels of *IL15*, and increased proliferating T cells were also found in the tumor center (Fig. 5D) in patients with high *IL15* expression. Similarly, a significantly higher density of proliferating B cells was found in the invasive margin of patients with high levels of *IL15* (Fig. 5C), and an increased density

Fig. 3. IL15 production within the tumor microenvironment and its impact on T cell proliferation and patient survival. (A) CRC sections were assessed immunohistochemically with mouse anti-human IL15 or corresponding isotype controls and counterstained with hematoxylin. Representative images of patients without genomic alterations of *IL15* (top panel) and with *IL15* deletion (lower panel).



Histograms represent means \pm SEM of IL15 intensity. Significantly different intensity is marked by "**." (C) Kaplan-Meier curves for DFS for patients having chromosomal deletion (green) of *IL15* versus patients without genetic alterations (black). (D) In situ hybridization was used to evaluate IL15-producing cells on consecutive slides of CRC tumors. (E) Representative images of single enzymatic staining of AE1AE3 [alkaline phosphatase (APS), blue] and IL15 [3,3'-diaminobenzidine (DAB), brown] with counterstain. Tumor cells producing IL15 were illustrated using double staining of IL15 (DAB, brown) with AE1AE3 (APS, blue). Double staining of IL15 (DAB, brown) with CD3 (APS, blue) was also illustrated, indicating no IL15-producing CD3 cells. (F) Triple immunofluorescence of IL15 (Cy3, red) was achieved with AE1AE3 [fluorescein isothiocyanate (FITC), green] and CD3 (AF647, white). Slides were mounted using 4',6-diamidino-2-phenylindole (DAPI) (blue)-containing mounting medium. A composite image of all four channels is illustrated. (G) IL15 biological roles, related genes based on experimental data, and in silico information and targeting miRNAs were revealed with CluePedia. The circular nodes represent pathways and functions of IL15. The top 10 genes correlating with IL15 ($r > 0.6$) on the basis of Affymetrix data from cohort 2 are shown in yellow. The top 10 predicted genes (STRING combined score >0.8) and 3'UTR-binding miRNAs (miRWalk) are shown in red and green, respectively. The links between the nodes are based on κ score. (H) T cell proliferation within CRC tumors was measured as the number of CD3⁺Ki67⁺ cells/mm² of tissue. The center of the tumor (CT), the invasive margin (IM), and the lymphoid islets (LI) in patients with (green) and without *IL15* deletion (white) were investigated. Histograms represent the mean densities \pm SEM of proliferating T cells (*** $P < 0.005$, ** $0.005 > P < 0.01$, * $0.01 > P < 0.05$).

of proliferating B cells was observed in the lymphoid islets and tumor center (Fig. 5, B and D). These results indicated that a decreased *IL15* expression in CRC tumors might affect the proliferation status of B and T lymphocytes. Subsequently, we stratified the patients into two groups according to their B and T cell proliferation status (high or low) using an unsupervised hierarchical clustering method. Log-rank analysis showed that patients with high densities of proliferating T and B cells in the lymphoid islets had a lower risk of relapse compared to those with low density; however, the difference in disease-free survival (DFS) was not significant (Fig. 5E). Patients with a low density of proliferative T and B cells in the tumor center and invasive margin had a significantly higher risk to relapse compared to those with high density of these cells (Fig. 5F). These results underline the importance of the presence and localization of proliferative T and B cells within the tumor microenvironment.

DISCUSSION

Given the major importance of the local immune reaction at the tumor site (1–3, 39) and of the immune contexture (40, 41), it is critical to understand mechanisms resulting in high or low densities of specific immune cells within the tumor. We previously demonstrated that the local presence of specific chemokines and adhesion molecules is associated with high or low densities of specific immune cells at the tumor site (42), suggesting that lymphocyte attraction and adhesion are critical processes. In addition to those mechanisms, genomic alterations that occur in neoplastic cells during tumor development and progression could influence the tumor microenvironment. This study presents a comprehensive analysis of cytokines, important players in the tumor-immune infiltrate crosstalk, in a large cohort of CRC tumors. The combination of large-scale data analysis with a systems biology approaches facilitated an in-depth exploration into the impact of genomic alterations in different cytokine families.

We showed that cytokine genes located in close proximity on chromosomes share similar genomic alterations. Aberrations affecting an extended genomic region could therefore affect the entire cytokine clusters with important functional consequences. Although the vast majority of CRC patients did not show gains or losses of cytokine genes, subgroups of patients with particular cytokine gene aberrations could be defined. There is a complex relationship between the DNA content and the perturbation of gene expression

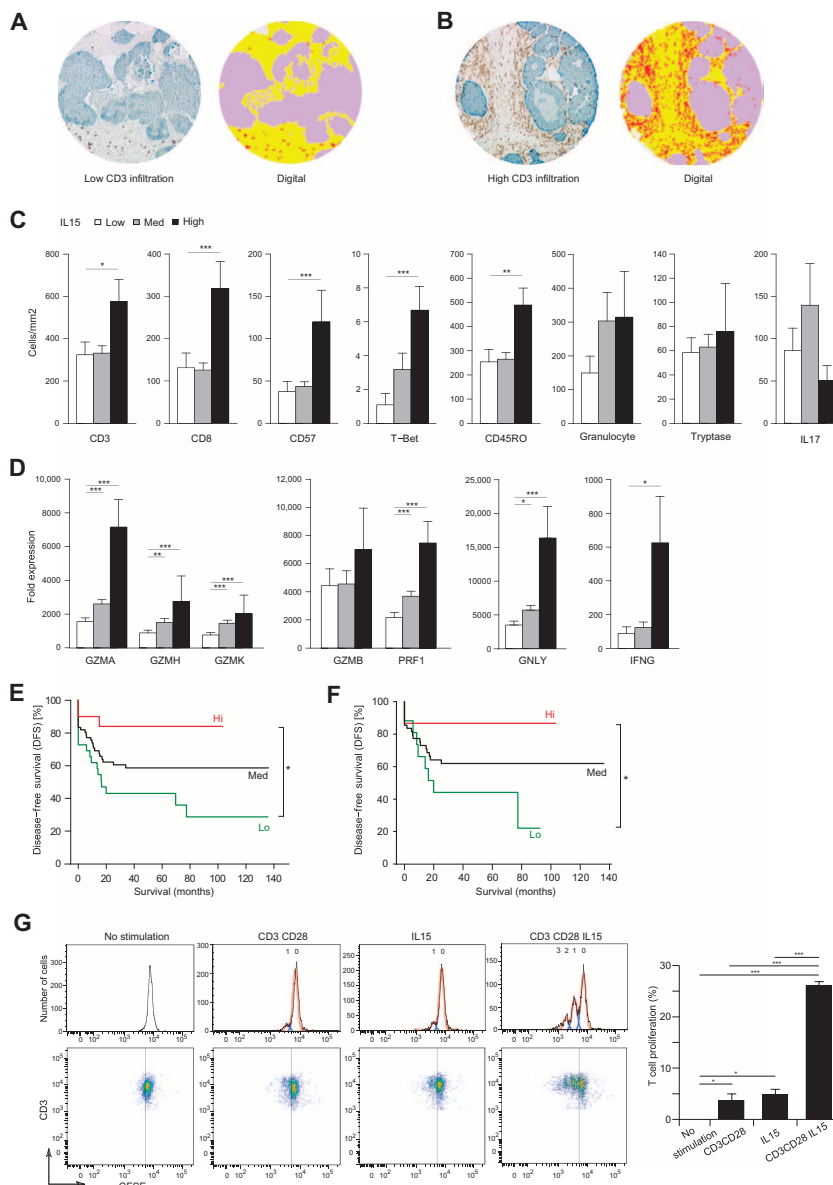


Fig. 4. *IL15* expression and the modulation of immune cell density within CRCs. (A and B) Two CRC patients with low (A) and high (B) *IL15* expression were assessed immunohistochemically for CD3⁺ cell infiltration (brown) and tumor marker (blue) (left). The digital quantification is shown on the right: tissue (yellow), tumor (purple), and CD3⁺ cells (red). (C) Immune marker densities were measured by tissue microarray in groups of patients with low (white), median (gray), and high (black) *IL15* expression. Histograms represent the mean density \pm SEM of T cells (CD3), cytotoxic T cells (CD8), activated T/NK cells (CD57), T_H1 cells (T-Bet), memory T cells (CD45RO), neutrophils (Granulocyte), mast cells (Tryptase), and T_H17 (IL17). Statistical analyses were performed with the Wilcoxon-Mann-Whitney method ($***P < 0.005$, $**0.005 > P < 0.01$, $*0.01 > P < 0.05$). (D) Immune marker expression levels were measured by qPCR in groups of patients with low (white), median (gray), and high (black) *IL15* expression. Histograms represent the mean expression level \pm SEM of effector T cell, cytotoxic, and T_H1 genes. Statistical analyses were performed with the Wilcoxon-Mann-Whitney method ($***P < 0.005$, $**0.005 > P < 0.01$, $*0.01 > P < 0.05$). (E and F) Kaplan-Meier curves for DFS for patients with high (red), medium (green), and low (black) *IL15* expression. (F) Patients having chromosomal deletion of *IL15* were excluded from this analysis. $***P < 0.005$, $**0.005 > P < 0.01$, $*0.01 > P < 0.05$, log-rank test. (G) Representative fluorescence-activated cell sorting (FACS) plots illustrating the T cell proliferation under different stimulation conditions. One-way analysis of variance (ANOVA) followed by Tukey's multiple comparison test was applied ($***P < 0.005$, $**0.005 > P < 0.01$, $*0.01 > P < 0.05$).

(24, 43). IL6, an inflammatory cytokine previously reported to be up-regulated in serum and tumor samples of humans and mice suffering from breast, prostate, lung, liver, and colon cancer (44–46), was amplified in 40% of the CRC patients, but its expression level was similar in patients with or without gain. Those patient groups also had comparable DFS. Different mechanisms could be involved in the regulation of cytokine expression, and other cells besides immune cells could produce such cytokines. Similar results were obtained for *IL28RA*, the most frequently deleted cytokine receptor. The lack of correlation between the expression of a gene and the genomic alterations of the region where the gene resides could involve other gene expression regulation mechanisms, including mutation, methylation, and miRNA expression.

Multiple genetic events accumulate during tumor progression (47); however, we found a similar profile of cytokine aberrations in tumor stages T1, T2, T3, and T4 (Fig. 1E). In contrast, an overrepresentation of *IL2*, *IL8*, *IL15*, and *IL21* deletions was seen in metastatic patients, indicating that those ILs may be involved in protective, antitumoral immune mechanisms. We investigated changes of cytokine expression in groups of patients with aberrations and their impact on survival. Patients with amplification displayed higher expression in genes located in chromosomes 4q26–27, 9p22, and 21q22, regions reported to be associated with ovarian cancer development and overall survival (48, 49) and pancreatic cancer susceptibility (50). Within those regions, clusters of IFN genes showed increased expression in amplified patients but without impact on CRC patient survival. Other cytokines from 4q26–27, *IL21* and *IL2*, showed higher expression in three amplified patients. However, the incidence of *IL21* and *IL2* deletion in the cohort was higher than the amplification and had a negative impact on patient survival. In CRC, the deletion of 4q26 has been reported to occur preferentially in microsatellite-stable patients (51). *IFNAR1* was the only cytokine for which both gain and loss were reflected in significant differences in gene expression level compared to patients without aberrations. Located close on 21q22, *IL10RB* also showed a significantly lower expression in deleted patients, similarly to *IL9* at 5q31.1 and *IL15* from 4q31. These deletions had no impact on the survival of patients. In contrast, besides *IL2* and *IL21*, patients with deletions of *IL12RB1* and *IL15* had a significantly different risk to relapse compared to those without aberrations.

Broad deletions of chromosome 4 (4p) have been previously shown to be associated with survival in CRC patients. No oncogene or tumor suppressor gene was located in this region (23), although *FBXW7* from 4p has been described as a tumor suppressor gene implicated in the control of chromosome stability (52, 53).

IL15 was the only cytokine with a significant impact on survival and displayed concordant copy number variation and gene expression level. This underlines the major role of *IL15* in human cancer. Patients with deletion at the *IL15* locus showed low expression of *IL15* and had a higher risk of relapse compared to those without aberrations. The ex vivo proliferation status of T cells alludes to the possibility that increases in *IL15* within the tumor microenvironment could result in a local increase in T cell proliferation. Subsequently, *IL15*-deleted patients had a lower density of proliferating immune cells

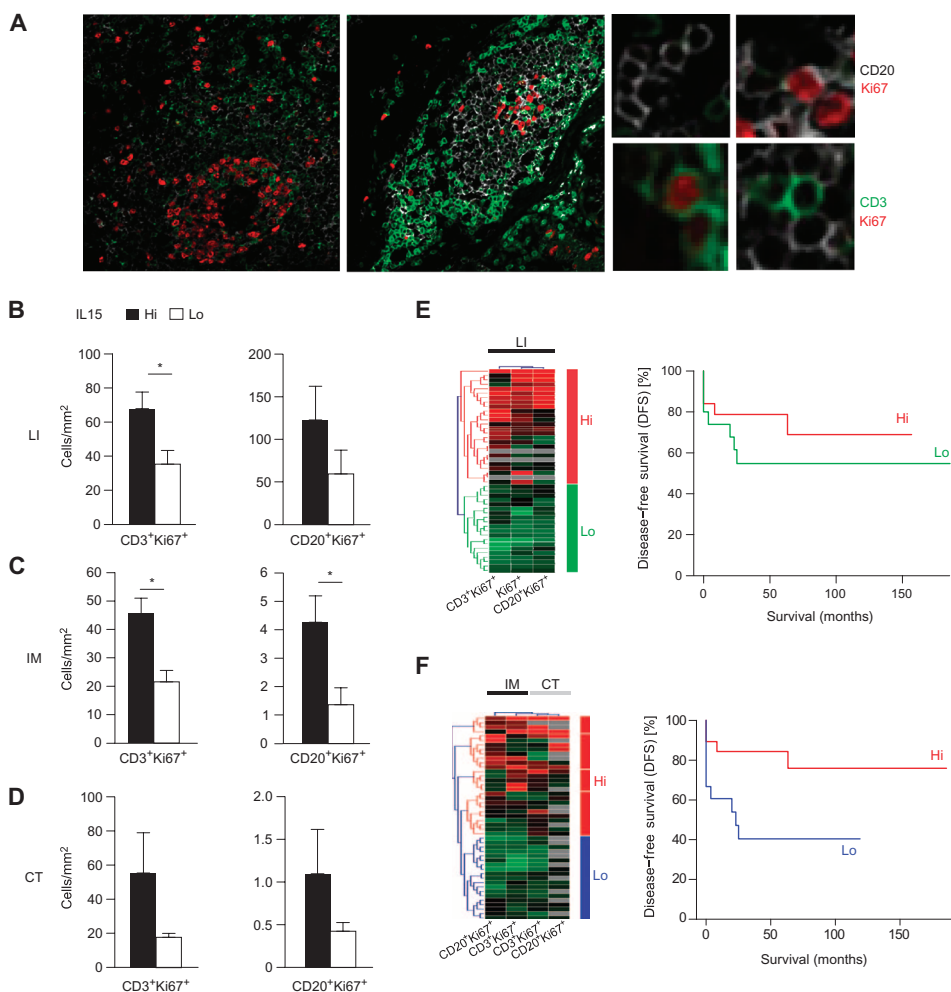


Fig. 5. IL15 and the intratumoral immune reaction. (A) T (CD3⁺) and B (CD20⁺) cell proliferation within CRCs. CD3⁺, CD20⁺, and Ki67⁺ cells are shown in green, gray, and red, respectively. (B to D) Histograms represent the mean densities \pm SEM of lymphocytes (CD3⁺Ki67⁺ and CD20⁺Ki67⁺) as the number of positive cells/mm² of tissue in the (B) lymphoid islets (LI), (C) invasive margin (IM), and (D) center of the tumor (CT) from CRC patients. The mean density in patients with high and low expression of *IL15* is shown in black and white columns. Significantly different density is marked by ^{*}, ^{**}. (E and F) Proliferation data from LI (E) and from IM and CT (F) were normalized and hierarchical clustered (Euclidean algorithm, Complete Linkage) in Genesis (57). High density of proliferative cells is shown in red, and low density in green. Missing data are represented in gray. Two patient clusters were revealed. Kaplan-Meier curves for DFS show the risk to relapse of patients with high (red) and low [(E) green; (F) blue] density of proliferative cells.

within the tumor (fig. S2). These results are concordant with the ability of *IL15* to activate important mechanisms of antitumor immunity (54), including development and activity of T and NK cells and promoting a persistent immune response through its action on memory T cells (38). Among all cytokine and cytokine receptor family members, deletion of *IL15* at the genomic level in CRC may be one of the main mechanisms explaining decreased proliferation of T and B cells within the tumor, in particular in lymphoid islets and at the invasive margin. Thus, *IL15* expression changes the intratumoral immune contexture (40, 41) and Immunoscore (15, 55) in CRC. Among all means of escape, deletion of *IL15* may be one of the major immune mechanisms associated with decreased T and B cells in human CRC.

IL15 participates in the development of important immune anti-tumor mechanisms, and it has therefore a great potential to be used in tumor immunotherapy (7). The results reported here shed a new light on the role of cytokines in CRC, show the clinical significance of cytokine levels in cancer, and demonstrate the importance of active intratumoral lymphocyte proliferation for the survival of the patients. Our findings represent major progress toward improving cancer patient prognosis using *IL15* biomarker, and the potential of *IL15* as target for immunotherapeutic treatment of cancer.

MATERIALS AND METHODS

Study design

The tissue sample material was collected at the Laennec–HEGP Hospitals (Hôpital Européen Georges Pompidou). A secure Web-based database, TME.db, was built for the management of the patient data. Ethical, legal, and social implications were approved by the ethical review board. The clinical characteristics of the cohorts used are described in table S5. No significant difference (Fisher's exact test) between cohorts was observed. The observation time in the cohorts was the interval between diagnosis and last contact (death or last follow-up). Data were censored at the last follow-up for patients without relapse or death. Time to recurrence or disease-free time was defined as the interval from the date of surgery to confirmed tumor relapse date for relapsed patients, and from the date of surgery to the date of last follow-up for disease-free patients.

Statistical analysis

The *t* test and the Wilcoxon-Mann-Whitney test were the parametric and nonparametric tests used to identify markers with a significantly different expression among patient groups. Kaplan-Meier curves were used to visualize survival differences. Significant difference of DFS among patient groups was calculated with the log-rank test. *P* values were corrected with the method proposed by Altman *et al.* We used a multivariate Cox proportional hazards model to determine hazard ratios. All tests were two-sided, and *P* < 0.05 was considered statistically significant. All analyses were performed with TME.db (56) and R statistical software (survival package).

Array CGH

Samples were homogenized (ceramic beads and FastPrep-24, MP Biomedicals) in lysis buffer [1 M tris, 0.5 M EDTA (pH 8), 20% SDS, proteinase K] and incubated overnight at 37°C. Genomic DNA was extracted by phenol-chloroform extraction and ethanol precipitation. Genomic DNA was resuspended in highly pure water. Concentrations

were evaluated by optical density measurement. Samples were labeled with a BioPrime Array CGH Genomic Labeling Kit according to the manufacturer's instructions (Invitrogen). Test DNA and reference DNA (500 ng) (Promega) were differentially labeled with deoxycytidine triphosphate (dCTP)-Cy5 and dCTP-Cy3, respectively (GE Healthcare). aCGH was carried out with a whole-genome oligonucleotide microarray platform (Human Genome CGH 44B Microarray Kit, Agilent Technologies). Slides were scanned with a microarray scanner (G2505B), and images were analyzed with CGH Analytics software 3.4.40 (both from Agilent Technologies). Along the chromosomes, the frequency in the cohort and the mean amplitude of the gain of each gene were used to calculate an amplification score (score = frequency × amplitude). In the same way, a deletion score was calculated.

RNA extraction

Tissue samples were snap-frozen within 15 min after surgery and stored in liquid nitrogen. From this material, 153 frozen tumor specimens were randomly selected for RNA extraction. The total RNA was isolated by homogenization with the RNeasy isolation kit (Qiagen). A bioanalyzer (Agilent Technologies) was used to evaluate the integrity and the quantity of the RNA.

Low-density array real-time TaqMan qPCR analysis

Fifty-nine cytokines and seven T cell effector markers were tested with real-time TaqMan analysis. The quantitative reverse transcription PCR experiments were all performed according to the manufacturer's instructions (Applied Biosystems). The quantitative real-time TaqMan qPCR analysis was performed with low-density arrays and the 7900 Robotic Real-Time PCR System (Applied Biosystems). As internal control, 18S ribosomal RNA primers and probes were used. The data were analyzed with the SDS software v2.2 (Applied Biosystems) and TME.db statistical module.

Affymetrix gene chip analysis

From this RNA, 105 Affymetrix gene chips were done with the HG-U133A GeneChip 3' IVT Express Kit. The raw data were normalized with the GCRMA algorithm. Finally, the log₂ intensities of the gene expression data were used for further analysis.

Immunohistochemistry

Formalin-fixed, paraffin-embedded (FFPE) CRC sections (4 μm) from tumors with and without *IL15* deletion were assessed immunohistochemically. After antigen retrieval (tris-EDTA, pH 9), quenching of endogenous peroxidase activity was achieved with 3% H₂O₂. Sections were treated with serum-free protein block (Dako) before a 60-min incubation with mouse anti-human *IL15* (Abcam, 3 μg/ml) or corresponding isotype controls and counterstained with hematoxylin. Double enzymatic or triple fluorescence staining of *IL15* was achieved with mouse anti-human cytokeratin (AE1/AE3, Dako, 2.16 μg/ml) and polyclonal rabbit anti-human CD3 (Dako, 7.5 μg/ml). Enzymatic revelation was achieved with red AEC Peroxidase Substrate Kit, blue Alkaline Phosphatase Substrate Kit III (Vector Laboratories), and brown DAB Chromogen System (Dako). Fluorescent slides were visualized with anti-mouse FITC (Sigma-Aldrich), anti-rabbit AF647, and streptavidin-Cy3 (Jackson ImmunoResearch) and mounted with DAPI-containing ProLong medium (Invitrogen). Slides were viewed on a Zeiss Axiovert 200 M microscope, and images were captured with an AxioCam MRm camera (×16).

In situ hybridization

Consecutive 5- μ m CRC sections were prepared and dewaxed under ribonuclease-free conditions. After antigen retrieval, tissue was digested with protease at 40°C for 20 min. In situ hybridizations were performed with target-specific probes (QuantiGene, ViewRNA ISH Tissue 2-Plex Assay, Affymetrix). Slides were dried and mounted with Vectashield mounting medium H1000 (Vector Laboratories) and observed under fluorescence with a Leica DMRB microscope ($\times 20$).

Ex vivo immune cell proliferation by flow cytometry

Ex vivo proliferation was measured with carboxyfluorescein diacetate succinimidyl ester (CFSE) dilution and flow cytometry. After mechanical dispersion, cells from fresh tumor sample were washed and labeled with CFSE (Molecular Probes) at a final concentration of 5 μ M for 10 min. Washed, counted, and viable cells were seeded in triplicate in 96-well flat-bottomed plates at a concentration of 4×10^5 cells per well. Cells were incubated in plates precoated with CD3 (5 μ g/ml) and CD28 antibodies (1 μ g/ml). Cells were cultured for 3 or 5 days \pm recombinant human IL15 (10 ng/ml, RD Systems) before the assessment of their CFSE-determined proliferation status. Cells were stained with CD3-AF700 (BD Biosciences) and fixed in 1% paraformaldehyde (Leiden University Medical Center pharmacy). Analyses were performed with a FACS Fortessa flow cytometer and FlowJo software (Tree Star).

In situ immune cell proliferation

Fluorescence immunohistochemistry on FFPE CRC sections was used to investigate the tumor center, invasive margin, and lymphoid islets. Triple staining facilitated quantification of proliferating B (CD20⁺Ki67⁺) and T (CD3⁺Ki67⁺) cells. Quantification of cell densities was performed (Definiens). Proliferation data were normalized and hierarchical clustered (Euclidean algorithm, Complete Linkage) in Genesis (57).

Functional analysis and predictions with ClueGO/CluePedia

Experimental and in silico data were integrated with ClueGO (27) and CluePedia (26) plug-ins of Cytoscape (32). ClueGO functional analyses were performed. CluePedia was used to predict genes associated to cytokines and miRNA–target gene pairs on the basis of STRING (33) and miRWalk (30) information, respectively. Correlations between *IL15* and Affymetrix tested genes were calculated with CluePedia. The top 10 predicted and top 10 correlating genes ($r > 0.6$) were included in the network together with the top 10 scored miRNAs. The Organic algorithm that determines the node positions on the basis of their connectivity was used for laying out the network.

SUPPLEMENTARY MATERIALS

www.sciencetranslationalmedicine.org/cgi/content/full/6/228/228ra37/DC1

Fig. S1. Cell types expressing *IL15*.

Fig. S2. Schematic representation of *IL15* impact on immune cell proliferation within tumors.

Table S1. Cytokines investigated in CRC: Families and the chromosomal location.

Table S2. Genomic alterations of cytokines in CRC.

Table S3. Genomic alterations of cytokines in relation with metastasis of CRC patients.

Table S4. The impact of genomic alterations of cytokines on the gene expression and the CRC patient disease-free survival.

Table S5. Clinical characteristics of the cohorts investigated.

REFERENCES AND NOTES

- J. Galon, A. Costes, F. Sanchez-Cabo, A. Kirilovsky, B. Mlecnik, C. Lagorce-Pagès, M. Tosolini, M. Camus, A. Berger, P. Wind, F. Zinzindohoué, P. Bruneval, P. H. Cugnenc, Z. Trajanoski, W. H. Fridman, F. Pagès, Type, density, and location of immune cells within human colorectal tumors predict clinical outcome. *Science* **313**, 1960–1964 (2006).
- B. Mlecnik, M. Tosolini, A. Kirilovsky, A. Berger, G. Bindea, T. Meatchi, P. Bruneval, Z. Trajanoski, W. H. Fridman, F. Pagès, J. Galon, Histopathologic-based prognostic factors of colorectal cancers are associated with the state of the local immune reaction. *J. Clin. Oncol.* **29**, 610–618 (2011).
- F. Pagès, A. Kirilovsky, B. Mlecnik, M. Asslaber, M. Tosolini, G. Bindea, C. Lagorce, P. Wind, F. Marliot, P. Bruneval, K. Zatloukal, Z. Trajanoski, A. Berger, W. H. Fridman, J. Galon, In situ cytotoxic and memory T cells predict outcome in patients with early-stage colorectal cancer. *J. Clin. Oncol.* **27**, 5944–5951 (2009).
- O. J. Finn, Cancer immunology. *N. Engl. J. Med.* **358**, 2704–2715 (2008).
- D. Wang, R. N. Dubois, A. Richmond, The role of chemokines in intestinal inflammation and cancer. *Curr. Opin. Pharmacol.* **9**, 688–696 (2009).
- G. Dranoff, Cytokines in cancer pathogenesis and cancer therapy. *Nat. Rev. Cancer* **4**, 11–22 (2004).
- E. Vacchelli, L. Galluzzi, A. Eggermont, J. Galon, E. Tartour, L. Zitvogel, G. Kroemer, Trial Watch: Immunostimulatory cytokines. *Oncimmunology* **1**, 493–506 (2012).
- J. M. González-Navajas, J. Lee, M. David, E. Raz, Immunomodulatory functions of type I interferons. *Nat. Rev. Immunol.* **12**, 125–135 (2012).
- E. D. Thompson, H. L. Enriquez, Y. X. Fu, V. H. Engelhard, Tumor masses support naive T cell infiltration, activation, and differentiation into effectors. *J. Exp. Med.* **207**, 1791–1804 (2010).
- E. Wang, M. C. Panelli, V. Monsurró, F. M. Marincola, A global approach to tumor immunology. *Cell. Mol. Immunol.* **1**, 256–265 (2004).
- R. Bonecchi, M. Locati, A. Mantovani, Chemokines and cancer: A fatal attraction. *Cancer Cell* **19**, 434–435 (2011).
- R. D. Schreiber, L. J. Old, M. J. Smyth, Cancer immunoeediting: Integrating immunity's roles in cancer suppression and promotion. *Science* **331**, 1565–1570 (2011).
- H. K. Angell, J. Galon, From the immune contexture to the Immunoscore: The role of prognostic and predictive immune markers in cancer. *Curr. Opin. Immunol.* **25**, 261–267 (2013).
- J. Galon, H. K. Angell, D. Bedognetti, F. M. Marincola, The continuum of cancer immunosurveillance: Prognostic, predictive, and mechanistic signatures. *Immunity* **39**, 11–26 (2013).
- J. Galon, F. Pagès, F. M. Marincola, H. K. Angell, M. Thurin, A. Lugli, I. Zlobec, A. Berger, C. Bifulco, G. Botti, F. Tatangelo, C. M. Britten, S. Kreiter, L. Chouchane, P. Delrio, H. Arndt, M. Asslaber, M. Maio, G. V. Masucci, M. Mihm, F. Vidal-Vanaclocha, J. P. Allison, S. Gnjatic, L. Hakansson, C. Huber, H. Singh-Jasuja, C. Ottensmeier, H. Zwierina, L. Laghi, F. Grizzi, P. S. Ohashi, P. A. Shaw, B. A. Clarke, B. G. Wouters, Y. Kawakami, S. Hazama, K. Okuno, E. Wang, J. O'Donnell-Tormey, C. Lagorce, G. Pawelec, M. I. Nishimura, R. Hawkins, R. Lapointe, A. Lundqvist, S. N. Khleif, S. Ogino, P. Gibbs, P. Waring, N. Sato, T. Torigoe, K. Itoh, P. S. Patel, S. N. Shukla, R. Hakansson, I. D. Nagtegaal, Y. Wang, C. D'Arrigo, S. Kopetz, F. A. Sinicrope, G. Trinchieri, T. F. Gajewski, P. A. Ascierto, B. A. Fox, Cancer classification using the Immunoscore: A worldwide task force. *J. Transl. Med.* **10**, 205 (2012).
- M. Tosolini, A. Kirilovsky, B. Mlecnik, T. Fredriksen, S. Mauger, G. Bindea, A. Berger, P. Bruneval, W. H. Fridman, F. Pagès, J. Galon, Clinical impact of different classes of infiltrating T cytotoxic and helper cells (Th1, Th2, Treg, Th17) in patients with colorectal cancer. *Cancer Res.* **71**, 1263–1271 (2011).
- D. Hanahan, R. A. Weinberg, Hallmarks of cancer: The next generation. *Cell* **144**, 646–674 (2011).
- J. T. Bensen, P. A. Dawson, J. C. Mychaleckyj, D. W. Bowden, Identification of a novel human cytokine gene in the interleukin gene cluster on chromosome 2q12-14. *J. Interferon Cytokine Res.* **21**, 899–904 (2001).
- H. Fickenscher, S. Hör, H. Küpers, A. Knappe, S. Wittmann, H. Sticht, The interleukin-10 family of cytokines. *Trends Immunol.* **23**, 89–96 (2002).
- T. B. Shownk, A. Y. Sakaguchi, S. L. Naylor, D. V. Goedell, R. M. Lawn, Clustering of leukocyte and fibroblast interferon genes of human chromosome 9. *Science* **218**, 373–374 (1982).
- B. H. van Leeuwen, M. E. Martinson, G. C. Webb, I. G. Young, Molecular organization of the cytokine gene cluster, involving the human IL-3, IL-4, IL-5, and GM-CSF genes, on human chromosome 5. *Blood* **73**, 1142–1148 (1989).
- H. Aragane, C. Sakakura, M. Nakanishi, R. Yasuoka, Y. Fujita, H. Taniguchi, A. Hagiwara, T. Yamaguchi, T. Abe, J. Inazawa, H. Yamagishi, Chromosomal aberrations in colorectal cancers and liver metastases analyzed by comparative genomic hybridization. *Int. J. Cancer* **94**, 623–629 (2001).
- M. Sheffer, M. D. Bacolod, O. Zuk, S. F. Giardina, H. Pincas, F. Barany, P. B. Paty, W. L. Gerald, D. A. Notterman, E. Domany, Association of survival and disease progression with chromosomal instability: A genomic exploration of colorectal cancer. *Proc. Natl. Acad. Sci. U.S.A.* **106**, 7131–7136 (2009).
- D. Tsafir, M. Bacolod, Z. Selvanayagam, I. Tsafir, J. Shia, Z. Zeng, H. Liu, C. Krier, R. F. Stengel, F. Barany, W. L. Gerald, P. B. Paty, E. Domany, D. A. Notterman, Relationship of gene expression and chromosomal abnormalities in colorectal cancer. *Cancer Res.* **66**, 2129–2137 (2006).

25. A. Bagchi, A. A. Mills, The quest for the 1p36 tumor suppressor. *Cancer Res.* **68**, 2551–2556 (2008).
26. G. Bindea, J. Galon, B. Mlecnik, CluePedia Cytoscape plugin: Pathway insights using integrated experimental and in silico data. *Bioinformatics* **29**, 661–663 (2013).
27. G. Bindea, B. Mlecnik, H. Hackl, P. Charoentong, M. Tosolini, A. Kirilovsky, W. H. Fridman, F. Pagès, Z. Trajanoski, J. Galon, ClueGO: A Cytoscape plug-in to decipher functionally grouped gene ontology and pathway annotation networks. *Bioinformatics* **25**, 1091–1093 (2009).
28. M. Ashburner, C. A. Ball, J. A. Blake, D. Botstein, H. Butler, J. M. Cherry, A. P. Davis, K. Dolinski, S. S. Dwight, J. T. Eppig, M. A. Harris, D. P. Hill, L. Issel-Tarver, A. Kasarskis, S. Lewis, J. C. Matese, J. E. Richardson, M. Ringwald, G. M. Rubin, G. Sherlock, Gene ontology: Tool for the unification of biology. The Gene Ontology Consortium. *Nat. Genet.* **25**, 25–29 (2000).
29. D. Croft, G. O'Kelly, G. Wu, R. Haw, M. Gillespie, L. Matthews, M. Caudy, P. Garapati, G. Gopinath, B. Jassal, S. Jupe, I. Kalatskaya, S. Mahajan, B. May, N. Ndegwa, E. Schmidt, V. Shamovsky, C. Yung, E. Birney, H. Hermjakob, P. D'Eustachio, L. Stein, Reactome: A database of reactions, pathways and biological processes. *Nucleic Acids Res.* **39**, D691–D697 (2011).
30. H. Dweep, C. Sticht, P. Pandey, N. Gretz, miRNAWalk—Database: Prediction of possible miRNA binding sites by “walking” the genes of three genomes. *J. Biomed. Inform.* **44**, 839–847 (2011).
31. M. Kanehisa, S. Goto, S. Kawashima, A. Nakaya, The KEGG databases at GenomeNet. *Nucleic Acids Res.* **30**, 42–46 (2002).
32. M. E. Smoot, K. Ono, J. Ruscheinski, P. L. Wang, T. Ideker, Cytoscape 2.8: New features for data integration and network visualization. *Bioinformatics* **27**, 431–432 (2011).
33. D. Szklarczyk, A. Franceschini, M. Kuhn, M. Simonovic, A. Roth, P. Minguéz, T. Doerks, M. Stark, J. Müller, P. Bork, L. J. Jensen, C. von Mering, The STRING database in 2011: Functional interaction networks of proteins, globally integrated and scored. *Nucleic Acids Res.* **39**, D561–D568 (2011).
34. G. Bindea, B. Mlecnik, M. Tosolini, A. Kirilovsky, M. Waldner, A. C. Obenauf, H. Angell, T. Fredriksen, L. Lafontaine, A. Berger, P. Bruneval, W. H. Fridman, C. Becker, F. Pagès, M. R. Speicher, Z. Trajanoski, J. Galon, Spatiotemporal dynamics of intratumoral immune cells reveal the immune landscape in human cancer. *Immunity* **39**, 782–795 (2013).
35. T. Barrett, D. B. Troup, S. E. Wilhite, P. Ledoux, C. Evangelista, I. F. Kim, M. Tomashevsky, K. A. Marshall, K. H. Phillippy, P. M. Sherman, R. N. Muertter, M. Holko, O. Ayanbule, A. Yefanov, A. Soboleva, NCBI GEO: Archive for functional genomics data sets—10 years on. *Nucleic Acids Res.* **39**, D1005–D1010 (2011).
36. T. D. Pfister, W. C. Reinhold, K. Agama, S. Gupta, S. A. Khin, R. J. Kinders, R. E. Parchment, J. E. Tomaszewski, J. H. Doroshow, Y. Pommier, Topoisomerase I levels in the NCI-60 cancer cell line panel determined by validated ELISA and microarray analysis and correlation with indenoisoquinoline sensitivity. *Mol. Cancer Ther.* **8**, 1878–1884 (2009).
37. P. C. Wilkinson, F. Y. Liew, Chemoattraction of human blood T lymphocytes by interleukin-15. *J. Exp. Med.* **181**, 1255–1259 (1995).
38. M. Jakobisiak, J. Golab, W. Lasek, Interleukin 15 as a promising candidate for tumor immunotherapy. *Cytokine Growth Factor Rev.* **22**, 99–108 (2011).
39. F. Pagès, A. Berger, M. Camus, F. Sanchez-Cabo, A. Costes, R. Molitor, B. Mlecnik, A. Kirilovsky, M. Nilsson, D. Damotte, T. Meatchi, P. Bruneval, P. H. Cugnenc, Z. Trajanoski, W. H. Fridman, J. Galon, Effector memory T cells, early metastasis, and survival in colorectal cancer. *N. Engl. J. Med.* **353**, 2654–2666 (2005).
40. W. H. Fridman, F. Pagès, C. Sautès-Fridman, J. Galon, The immune contexture in human tumours: Impact on clinical outcome. *Nat. Rev. Cancer* **12**, 298–306 (2012).
41. J. Galon, W. H. Fridman, F. Pagès, The adaptive immunologic microenvironment in colorectal cancer: A novel perspective. *Cancer Res.* **67**, 1883–1886 (2007).
42. B. Mlecnik, M. Tosolini, P. Charoentong, A. Kirilovsky, G. Bindea, A. Berger, M. Camus, M. Gillard, P. Bruneval, W. H. Fridman, F. Pagès, Z. Trajanoski, J. Galon, Biomolecular network reconstruction identifies T-cell homing factors associated with survival in colorectal cancer. *Gastroenterology* **138**, 1429–1440 (2010).
43. P. Platzer, M. B. Uppender, K. Wilson, J. Willis, J. Lutterbaugh, A. Nosrati, J. K. Willson, D. Mack, T. Ried, S. Markowitz, Silence of chromosomal amplifications in colon cancer. *Cancer Res.* **62**, 1134–1138 (2002).
44. R. Cammarota, V. Bertolini, G. Pennesi, E. O. Bucci, O. Gottardi, C. Garlanda, L. Laghi, M. C. Barberis, F. Sessa, D. M. Noonan, A. Albin, The tumor microenvironment of colorectal cancer: Stromal TLR-4 expression as a potential prognostic marker. *J. Transl. Med.* **8**, 112 (2010).
45. K. Heikilä, S. Ebrahim, D. A. Lawlor, Systematic review of the association between circulating interleukin-6 (IL-6) and cancer. *Eur. J. Cancer* **44**, 937–945 (2008).
46. Y. Li, C. de Haar, M. Chen, J. Deuring, M. M. Gerrits, R. Smits, B. Xia, E. J. Kuipers, C. J. van der Woude, Disease-related expression of the IL6/STAT3/SOCS3 signalling pathway in ulcerative colitis and ulcerative colitis-related carcinogenesis. *Gut* **59**, 227–235 (2010).
47. M. S. Pino, D. C. Chung, The chromosomal instability pathway in colon cancer. *Gastroenterology* **138**, 2059–2072 (2010).
48. E. L. Goode, G. Chenevix-Trench, H. Song, S. J. Ramus, M. Notaridou, K. Lawrenson, M. Widschwendter, R. A. Vierkant, M. C. Larson, S. K. Kjaer, M. J. Birrer, A. Berchuck, J. Schildkraut, I. Tomlinson, L. A. Kiemeny, L. S. Cook, J. Gronwald, M. Garcia-Closas, M. E. Gore, I. Campbell, A. S. Whittemore, R. Sutphen, C. Phelan, H. Anton-Culver, C. L. Pearce, D. Lambrechts, M. A. Rossing, J. Chang-Claude, K. B. Moysich, M. T. Goodman, T. Dörk, H. Nevanlinna, R. B. Ness, T. Rafnar, C. Hogdall, E. Hogdall, B. L. Fridley, J. M. Cunningham, W. Sieh, V. McGuire, A. K. Godwin, D. W. Cramer, D. Hernandez, D. Levine, K. Lu, E. S. Iversen, R. T. Palmieri, R. Houlston, A. M. van Altena, K. K. Aben, L. F. Massuger, A. Brooks-Wilson, L. E. Kelemen, N. D. Le, A. Jakubowska, J. Lubinski, K. Medrek, A. Stafford, D. F. Easton, J. Tyrer, K. L. Bolton, P. Harrington, D. Eccles, A. Chen, A. N. Molina, B. N. Davila, H. Arango, Y. Y. Tsai, Z. Chen, H. A. Risch, J. McLaughlin, S. A. Narod, A. Ziogas, W. Brewster, A. Gentry-Maharaj, U. Menon, A. H. Wu, D. O. Stram, M. C. Pike; Wellcome Trust Case-Control Consortium, J. Beesley, P. M. Webb; Australian Cancer Study (Ovarian Cancer); Australian Ovarian Cancer Study Group; Ovarian Cancer Association Consortium (OCAC), X. Chen, A. B. Ekici, F. C. Thiel, M. W. Beckmann, H. Yang, N. Wentzensen, J. Lissowska, P. A. Fasching, E. Despiere, F. Amant, I. Vergote, J. Doherty, R. Hein, S. Wang-Gohrke, G. Lurie, M. E. Carney, P. J. Thompson, I. Runnebaum, P. Hillemanns, M. Dürst, N. Antonenkova, T. Bogdanova, A. Leminen, R. Butzow, T. Heikkinen, K. Stefansson, P. Sulem, S. Besenbacher, T. A. Sellers, S. A. Gayther, P. D. Pharoah; Ovarian Cancer Association Consortium (OCAC), A genome-wide association study identifies susceptibility loci for ovarian cancer at 2q31 and 8q24. *Nat. Genet.* **42**, 874–879 (2010).
49. M. Thomassen, K. M. Jochumsen, O. Mogensen, Q. Tan, T. A. Kruse, Gene expression meta-analysis identifies chromosomal regions involved in ovarian cancer survival. *Genes Chromosomes Cancer* **48**, 711–724 (2009).
50. C. Wu, X. Miao, L. Huang, X. Che, G. Jiang, D. Yu, X. Yang, G. Cao, Z. Hu, Y. Zhou, C. Zuo, C. Zhang, X. Zhang, Y. Zhou, X. Yu, W. Dai, Z. Li, H. Shen, L. Liu, Y. Chen, S. Zhang, X. Wang, K. Hai, J. Chang, Y. Liu, M. Sun, W. Cao, J. Gao, Y. Ma, X. Zheng, S. T. Cheung, Y. Jia, J. Xu, W. Tan, P. Zhao, T. Wu, C. Wang, D. Lin, Genome-wide association study identifies five loci associated with susceptibility to pancreatic cancer in Chinese populations. *Nat. Genet.* **44**, 62–66 (2012).
51. J. Camps, G. Armengol, J. del Rey, J. J. Lozano, H. Vauhkonen, E. Prat, J. Egozcue, L. Sumoy, S. Knuutila, R. Miró, Genome-wide differences between microsatellite stable and unstable colorectal tumors. *Carcinogenesis* **27**, 419–428 (2006).
52. J. H. Mao, J. Perez-Losada, D. Wu, R. Delrosario, R. Tsunematsu, K. I. Nakayama, K. Brown, S. Bryson, A. Balmain, *Fbxw7/Cdc4* is a p53-dependent, haploinsufficient tumour suppressor gene. *Nature* **432**, 775–779 (2004).
53. H. Rajagopalan, P. V. Jallepalli, C. Rago, V. E. Velculescu, K. W. Kinzler, B. Vogelstein, C. Lengauer, Inactivation of hCDC4 can cause chromosomal instability. *Nature* **428**, 77–81 (2004).
54. T. A. Waldmann, The biology of interleukin-2 and interleukin-15: Implications for cancer therapy and vaccine design. *Nat. Rev. Immunol.* **6**, 595–601 (2006).
55. J. Galon, B. Mlecnik, G. Bindea, H. K. Angell, A. Berger, C. Lagorce, A. Lugli, I. Zlobec, A. Hartmann, C. Bifulco, I. D. Nagtegaal, R. Palmqvist, G. V. Masucci, G. Botti, F. Tatangelo, P. Delrio, M. Maio, L. Laghi, F. Grizzi, M. Asslaber, C. D'Arrigo, F. Vidal-Vanaclocha, E. Zavadova, L. Chouchane, P. S. Ohashi, S. Hafezi-Bakhtiari, B. G. Wouters, M. Roehrl, L. Nguyen, Y. Kawakami, S. Hazama, K. Okuno, S. Ogino, P. Gibbs, P. Waring, N. Sato, T. Torigoe, K. Itoh, P. S. Patel, S. N. Shukla, Y. Wang, S. Kopetz, F. A. Sinicropo, V. Scricariu, P. A. Ascierto, F. M. Marincola, B. A. Fox, F. Pagès, Towards the introduction of the 'Immunoscore' in the classification of malignant tumors. *J. Pathol.* **232**, 199–209 (2013).
56. B. Mlecnik, F. Sanchez-Cabo, P. Charoentong, G. Bindea, F. Pagès, A. Berger, J. Galon, Z. Trajanoski, Data integration and exploration for the identification of molecular mechanisms in tumor-immune cells interaction. *BMC Genomics* **11** (Suppl. 1), S7 (2010).
57. A. Sturm, J. Quackenbush, Z. Trajanoski, Genesis: Cluster analysis of microarray data. *Bioinformatics* **18**, 207–208 (2002).

Funding: This work was supported by grants from the Institut National du Cancer, INSERM, Med-Immune, Qatar National Research Fund under its National Priorities Research Program award number NPRP09-1174-3-291, the European Commission (7FP, Geninca Consortium, grant 202230), Cancer Research for Personalized Medicine, Cancerpole Ile de France, the Paris Alliance of Cancer Research Institutes, and the LabEx Immuno-oncology. **Author contributions:** M.S.S., H.K.A., T.F., A.K., A.M.B., L.L., M.W., and M.T. acquired the tumor microenvironment data. A.C.O., T.F., A.R., and M.R.S. acquired the genomic data. B.M. and G.B. analyzed the data. B.M. and G.B. were responsible for correlation of clinical data. A.B. was responsible for clinical data. B.M., G.B., W.H.F., A.R., F.P., V.V.-A., M.R.S., and J.G. interpreted the data. J.G. designed and supervised the study. B.M., G.B., and J.G. wrote the manuscript. H.K.A., A.B., W.H.F., A.R., F.P., V.V.-A., and M.R.S. revised the manuscript. **Competing interests:** The authors declare that they have no competing interests.

Submitted 5 August 2013
Accepted 25 February 2014
Published 19 March 2014
10.1126/scitranslmed.3007240

Citation: B. Mlecnik, G. Bindea, H. K. Angell, M. S. Sasso, A. C. Obenauf, T. Fredriksen, L. Lafontaine, A. M. Bilocq, A. Kirilovsky, M. Tosolini, M. Waldner, A. Berger, W. H. Fridman, A. Rafii, V. Valge-Archer, F. Pagès, M. R. Speicher, J. Galon, Functional network pipeline reveals genetic determinants associated with in situ lymphocyte proliferation and survival of cancer patients. *Sci. Transl. Med.* **6**, 228ra37 (2014).



Functional Network Pipeline Reveals Genetic Determinants Associated with *in Situ* Lymphocyte Proliferation and Survival of Cancer Patients

Bernhard Mlecnik, Gabriela Bindea, Helen K. Angell, Maria Stella Sasso, Anna C. Obenaus, Tessa Fredriksen, Lucie Lafontaine, Amelie M. Bilocq, Amos Kirilovsky, Marie Tosolini, Maximilian Waldner, Anne Berger, Wolf Herman Fridman, Arash Rafii, Vii Valge-Archer, Franck Pagès, Michael R. Speicher and Jérôme Galon (March 19, 2014)

Science Translational Medicine 6 (228), 228ra37. [doi: 10.1126/scitranslmed.3007240]

Editor's Summary

There Goes the Neighborhood

Just as a new homeowner will remodel when moving into a house, a tumor also alters the local microenvironment. One of the least tumor-friendly things in the tumor microenvironment is the immune response. Mlecnik *et al.* now examine the network of changes to cytokines that contribute to shaping the intratumoral immune response in colorectal tumors.

The authors found changes in local expression of 13 cytokines. Deletion of one cytokine, interleukin 15, was associated with tumor recurrence and reduced patient survival, potentially by affecting the local proliferation of B and T cells. Their results show that chromosome instability contributes to the regulation of cytokines and downstream tumor immune response.

The following resources related to this article are available online at <http://stm.sciencemag.org>. This information is current as of August 27, 2016.

Article Tools	Visit the online version of this article to access the personalization and article tools: http://stm.sciencemag.org/content/6/228/228ra37
Supplemental Materials	" <i>Supplementary Materials</i> " http://stm.sciencemag.org/content/suppl/2014/03/17/6.228.228ra37.DC1
Related Content	The editors suggest related resources on <i>Science's</i> sites: http://stm.sciencemag.org/content/scitransmed/1/8/8ra19.full http://stm.sciencemag.org/content/scitransmed/6/223/223ra22.full http://stm.sciencemag.org/content/scitransmed/8/327/327ra26.full
Permissions	Obtain information about reproducing this article: http://www.sciencemag.org/about/permissions.dtl

Science Translational Medicine (print ISSN 1946-6234; online ISSN 1946-6242) is published weekly, except the last week in December, by the American Association for the Advancement of Science, 1200 New York Avenue, NW, Washington, DC 20005. Copyright 2016 by the American Association for the Advancement of Science; all rights reserved. The title *Science Translational Medicine* is a registered trademark of AAAS.